Hindawi
Mathematical Problems in Engineering
Volume 2019, Article ID 8424283, 19 pages
https://doi.org/10.1155/2019/8424283

Research Article

Stiffness Calculation Model of Thread Connection Considering Friction Factors

Shi-kun Lu,[1,2] **Deng-xin Hua**,[1] **Yan Li**,[1] **Fang-yuan Cui**,[1] **and Peng-yang Li**[1]

[1]*Xi'an University of Technology, Xi'an 710048, China*
[2]*Laiwu Vocational and Technical College, Laiwu 271100, China*

Correspondence should be addressed to Deng-xin Hua; dengxinhua@xaut.edu.cn and Yan Li; jyxy-ly@xaut.edu.cn

Received 9 September 2018; Revised 12 December 2018; Accepted 1 January 2019; Published 23 January 2019

Guest Editor: Yingyot Aue-u-lan

In order to design a reasonable thread connection structure, it is necessary to understand the axial force distribution of threaded connections. For the application of bolted connection in mechanical design, it is necessary to estimate the stiffness of threaded connections. A calculation model for the distribution of axial force and stiffness considering the friction factor of the threaded connection is established in this paper. The method regards the thread as a tapered cantilever beam. Under the action of the thread axial force, in the consideration of friction, the two cantilever beams interact and the beam will be deformed, these deformations include bending deformation, shear deformation, inclination deformation of cantilever beam root, shear deformation of cantilever beam root, radial expansion deformation and radial shrinkage deformation, etc.; calculate each deformation of the thread, respectively, and sum them, that is, the total deformation of the thread. In this paper, on the one hand, the threaded connection stiffness was measured by experiments; on the other hand, the finite element models were established to calculate the thread stiffness; the calculation results of the method of this paper, the test results, and the finite element analysis (FEA) results were compared, respectively; the results were found to be in a reasonable range; therefore, the validity of the calculation of the method of this paper is verified.

1. Introduction

The bolts connect the equipment parts into a whole, which is used to transmit force, moment, torque, or movement. The bolt connection is widely used in various engineering fields, such as aviation machine tools, precision instruments, etc. The precision of the threaded connection affects the quality of the equipment. Especially for high-end CNC machine tools, the precision of the thread connection is very high. Therefore, it is important to study the stiffness of the threaded connection to improve the precision of the device. Many researchers have conducted research in this area.

Dongmei Zhang et al. [1], propose a method which can compute the engaged screw stiffness, and the validity of the method was verified by FEA and experiments. Maruyama et al. [2] used the point matching method and the FEM, based on the experimental results of Boenick and the assumptions made by Fernlund [3] in calculating the pressure distribution between joint plates. Motash [4] assumed that the pressure distribution on any plane perpendicular to the bolt axis had zero gradient at $r = d_h/2$ and $r = r_o$, where it also vanishes. They mainly use numerical methods to calculate the influence of different parameters on the stiffness of bolted connections. Kenny B, Patterson E A. [5] introduced a method for measuring thread strains and stresses. Kenny B [6] et al. reviewed the distribution of loads and stresses in fastening threads. Miller D L et al. [7] established the spring model of thread force analysis and, combined with the mathematical theory, analyzed the stress of the thread and compared with the FEA results and experimental results to verify the correctness of the spring mathematical model. Wang W and Marshek K M. et al. [8] proposed an improved spring model to analyze the thread load distribution, compared the load distributions of elastic threads and yielding thread joints, and discussed the effect of the yield line on the load distribution. Wileman et al. [9] performed a two-dimensional (2D) FEA for members stiffness of joint connection. De Agostinis M et al. [10] studied the effect of lubrication on

thread friction characteristics or torque. Dario Croccolo et al. [11–13] studied the effect of Engagement Ratio (ER, namely, the thread length over the thread diameter) on the tightening and untightening torque and friction coefficient of threaded joints using medium strength threaded locking devices. Zou Q. et al. [14, 15] studied the use of contact mechanics to determine the effective radius of the bolted joint and also studied the effect of lubrication on friction and torque-tension relationship in threaded fasteners. Nassar S. A. et al. [16, 17] studied the thread friction and thread friction torque in thread connection. Nassar S. A. et al. [18, 19] also investigated the effects of tightening speed and coating on the torque-tension relationship and wear pattern in threaded fastener applications in order to improve the reliability of the clamping load estimation in bolted joints. Kopfer et al. [20] believe that suitable formulations should consider contact pressure and sliding speed; based on this, the contribution shows experimental examples for main uncertainties of frictional behavior during tightening with different material combinations (results from assembly test stand). Kenny B et al. [21] reviewed the distribution of load and stress in the threads of fasteners. Shigley et al. [22] presented an analytical solution for member stiffness, based on the work of Lehnhoff and Wistehuff [23]. Nasser [24], Musto and Konkle [25], Nawras [26], and Nassar and Abbound [27] also proposed mathematical model for the bolted-joint stiffness. Qin et al. [28] established an analytical model of bolted disk-drum joints and introduced its application to dynamic analysis of joint rotor. Liu et al. [29] conducted experimental and numerical studies on axially excited bolt connections.

There are also several authors that, starting from the nature of thread stiffness, from the perspective of thread deformation, established a mathematical model of the calculation of the distribution of thread axial force. The Sopwith method [30] and the Yamamoto method [31] received extensive recognition. The Sopwith method gave a method for calculating the axial force distribution of threaded connections. Yamamoto method can not only calculate the axial force distribution of threads but also calculate the stiffness of threaded connections. The assumption for Yamamoto method is that the load per unit width along the helix direction is uniformly distributed. In fact, for the three-dimensional (3D) helix thread, the load distribution is not uniform. Therefore, based on the Yamamoto method, Dongmei Zhang et al. [1] propose a method which can compute the engaged screw stiffness by considering the load distribution, and the validity of the method was verified by FEA and experiments. The method of Zhang Dongmei does not consider the influence of the friction coefficient of the thread contact surface. In fact, the friction coefficient of the contact surface of the thread connection has an influence on the distribution of the axial force of the thread and the stiffness of the thread. Therefore, we propose a new method which can compute the engaged screw stiffness more accurately by considering the effects of friction and the load distribution. The accuracy of the method was verified by the FEA and bolt tensile test. The flow chart of the article is shown in Figure 2.

2. Mathematical Model

2.1. Axial Load Distribution. According to Yamamoto [31], the thread is regarded as a cantilever beam, and the thread is deformed under axial force and preload. These deformations include the following (shown in Figure 3): thread bending deformation, thread shear deformation, thread root inclination deformation, thread root shear deformation, radial direction extended deformation, or radial shrinkage deformation.

For the *ISO* thread, the axial deformation of the thread at x at the axial unit width force w_z is thread bending deformation δ_1, thread shear deformation δ_2, thread root inclination deformation δ_3, thread root shear deformation δ_4, and radial direction extended deformation δ_5 (nut) or radial shrinkage deformation δ_5 (screw), and calculate these deformations of the thread, respectively, and then sum them, that is, the total deformation.

2.1.1. Bending Deformation. In the threaded connection, under the action of the load, the contact surface friction coefficient is μ, when the sliding force along the inclined plane is greater than the friction force along the inclined plane, the relative sliding occurs between the two inclined planes, and the axial unit width force (shown in Figure 3) is w_z; if the influence of the lead angle is ignored, the force per unit width perpendicular to the thread surface can be expressed as

$$w = \frac{w_z}{\mu \sin \alpha + \cos \alpha} \tag{1}$$

The force per unit width perpendicular to the thread surface can be decomposed into the x-direction component force and the y-direction component force, respectively

$$w \cos \alpha = \frac{w_z \cos \alpha}{\mu \sin \alpha + \cos \alpha} \tag{2}$$

and

$$w \sin \alpha = \frac{w_z \sin \alpha}{\mu \sin \alpha + \cos \alpha} \tag{3}$$

The friction generated along the slope is $w\mu$; i.e.,

$$w\mu = \frac{w_z \mu}{\mu \sin \alpha + \cos \alpha} \tag{4}$$

The force $w\mu$ is also decomposed into x-direction force and y-direction force, which are $\mu \sin \alpha$ and $\mu \cos \alpha$, respectively.

$$w\mu \sin \alpha = \frac{w_z \mu \sin \alpha}{\mu \sin \alpha + \cos \alpha} \tag{5}$$

$$w\mu \cos \alpha = \frac{w_z \mu \cos \alpha}{\mu \sin \alpha + \cos \alpha} \tag{6}$$

In the unit width, the thread is regarded as a rectangular variable-section cantilever beam. Under the action of the

above-mentioned force, the thread undergoes bending deformation, and the virtual work done by the bending moment $\overline{E}$ on the beam dy section is

$$\overline{E}d\theta = \overline{E}\frac{M_w}{E_b I(y)}dy \tag{7}$$

According to the principle of virtual work, the deflection δ_1 (see Figure 3(a)) of the beam subjected to the load is

$$\delta_1 = \int_0^c \frac{\overline{E}M_w}{E_b I(y)}dy \tag{8}$$

where $\overline{E}$ is the bending moment of the unit load beam. M_w is the bending moment of the beam under the actual load. $I(y)$ is the area moment of inertia of the beam at y. E_b is Young's Modulus of the material. c is the length of the beam. Here, the forces are assumed as acting on the mean diameter of the thread.

As shown in Figure 5, the height $h(y)$ of the beam section per unit width and the area moment of inertia $I(y)$ of the section can be expressed by using the function interpolation.

$$\begin{aligned} h(y) &= \left[1 + \frac{(\beta_1 - 1)(c - y)}{c}\right]h, \quad (0 \le y \le c) \\ I(y) &= \frac{1}{12}bh^3\left[1 + \frac{(\beta_1 - 1)(c - y)}{c}\right]^3, \quad (0 \le y \le c) \\ \beta_1 &= \frac{a}{h} \end{aligned} \tag{9}$$

where h is the beam end section height; b is the beam section width; β_1 is the beam root section height and the beam end section height ratio; see Figure 5.

From Figure 5, the bending moment of the beam is related to the y-axis component of w and $w\mu$, and these components cause the beam to bend; therefore, the analytical solution shows that the bending moment of the unit width beam subjected to the friction force and the vertical load of the thread surface is

$$\begin{aligned} M_w = \frac{w_z}{\mu\sin\alpha + \cos\alpha} \cdot \Big[&\cos\alpha \cdot c + \mu\sin\alpha \cdot c \\ &- \sin\alpha\left(\frac{a}{2} - c\tan\alpha\right) + \mu\cos\alpha\left(\frac{a}{2} - c\tan\alpha\right)\Big] \end{aligned} \tag{10}$$

Substituting (10) and (9) to (8) and integrating to obtain the analytical expression of the deflection δ_1 (shown in Figure 3(a)) of the cantilever beam with variable cross-section under load one has

$$\delta_1 = \frac{12M_w c^2}{E_b bh^3} \cdot \left[\frac{1}{2}\left(\frac{1}{\beta_1^2} + 1\right) - \frac{1}{\beta_1}\right] \cdot \frac{1}{(\beta_1 - 1)^2} \tag{11}$$

2.1.2. Shear Deformation. Assume that the distribution of shear stress on any section is distributed according to the parabola [31] and the deformation δ_2 (see Figure 3(b)) caused by the shear force within the width of unit 1 is

$$\begin{aligned} \delta_2 = \log_e\left(\frac{a}{b}\right) \cdot \frac{6(1+\nu)(\cos\alpha + \mu\sin\alpha)\cot\alpha}{5E_b} \\ \cdot \frac{w_z}{\mu\sin\alpha + \cos\alpha} \end{aligned} \tag{12}$$

2.1.3. Inclination Deformation of the Thread Root. Under the action of the load, the thread surface is subjected to a bending moment, and the root of the thread is tilted, as shown in Figure 3(c). Due to the inclination of the thread, axial displacement occurs at the point of action of the thread surface force, and the axial displacement can be expressed as [31]

$$\begin{aligned} \delta_3 = \frac{w_z}{\mu\sin\alpha + \cos\alpha} \cdot \frac{12c(1-\nu^2)}{\pi E_b a^2} \cdot \Big[&\cos\alpha \cdot c \\ &+ \mu\sin\alpha \cdot c - \sin\alpha\left(\frac{a}{2} - c\tan\alpha\right) \\ &+ \mu\cos\alpha\left(\frac{a}{2} - c\tan\alpha\right)\Big] \end{aligned} \tag{13}$$

2.1.4. Deformation due to Radial Expansion and Radial Shrinkage. According to the static analysis, the thread is subjected to radial force $w\sin\alpha - w\mu\cos\alpha$ (shown in Figure 4), and it is known from the literature [31] that the internal and external thread radial deformation (shown in Figure 3(d)) are

$$\delta_{4b} = (1 - \nu_b)\frac{d_p}{2E_b P}\tan\alpha \cdot \frac{w_z(\sin\alpha - \mu\cos\alpha)}{\mu\sin\alpha + \cos\alpha} \tag{14}$$

and

$$\begin{aligned} \delta_{4n} = \left(\frac{D_0^2 + d_p^2}{D_0^2 - d_p^2} + \nu_n\right)\frac{d_p}{2E_n P} \cdot \tan\alpha \\ \cdot \frac{w_z(\sin\alpha - \mu\cos\alpha)}{\mu\sin\alpha + \cos\alpha} \end{aligned} \tag{15}$$

2.1.5. Shear Deformation of the Root. Assuming that the shear stress of the root section is evenly distributed, the displacement of the O point in the x direction caused by the shear deformation (shown in Figure 3(e)) is the same as the displacement of the thread in the x direction; this displacement can be expressed as [31]

$$\begin{aligned} \delta_5 = \frac{w_z}{\mu\sin\alpha + \cos\alpha} \cdot \frac{2(1-\nu^2)\cdot(\cos\alpha + \mu\sin\alpha)}{\pi E_b} \\ \cdot \left\{\frac{P}{a}\log_e\left(\frac{P + a/2}{P - a/2}\right) + \frac{1}{2}\log_e\left(\frac{4P^2}{a^2} - 1\right)\right\} \end{aligned} \tag{16}$$

For ISO internal threads, the relationship between a, b, c, and pitch P is

$$\begin{aligned} a &= 0.833P \\ b &= 0.5P \\ c &= 0.289P \end{aligned} \tag{17}$$

Substituting (17) into (9), (10), (11), (12), (13), (14), and (16) one gets the relation

$$\delta_{1b} = 3.468\frac{M_{wb}}{E_b P^2 \beta_b^3} \cdot \left[\frac{1}{2}\left(\frac{1}{\beta_b^2}+1\right) - \frac{1}{\beta_b}\right] \cdot \frac{1}{(\beta_b - 1)^2}, \quad \beta_b = 1.6684 \tag{18}$$

$$M_{wb} = \frac{w_z}{\mu \sin\alpha + \cos\alpha}\left[0.289P \cdot (\cos\alpha + \mu \cdot \sin\alpha) - (0.4165P - 0.289P \cdot \tan\alpha)(\sin\alpha - \mu \cdot \cos\alpha)\right] \tag{19}$$

$$\delta_{2b} = 0.51 \cdot \frac{6(1+\nu)(\cos\alpha + \mu\sin\alpha)\cot\alpha}{5E_b} \cdot \frac{w_z}{\mu\sin\alpha + \cos\alpha} \tag{20}$$

$$\delta_{3b} = \frac{w_z}{\mu\sin\alpha + \cos\alpha} \cdot \frac{12c\left(1-\nu^2\right)}{\pi E_b a^2} \cdot \left[0.289P \cdot (\cos\alpha + \mu\cdot\sin\alpha) - (0.4165P - 0.289P\cdot\tan\alpha) \cdot (\sin\alpha - \mu\cdot\cos\alpha)\right] \tag{21}$$

$$\delta_{4b} = (1-\nu_b)\frac{d_p}{2E_b P}(\sin\alpha - \mu\cos\alpha)\tan\alpha \cdot \frac{w_z}{\mu\sin\alpha + \cos\alpha} \tag{22}$$

$$\delta_{5b} = \frac{1.8449 w_z}{\mu\sin\alpha + \cos\alpha} \cdot \frac{2\left(1-\nu^2\right)\cdot(\cos\alpha + \mu\sin\alpha)}{\pi E_b} \tag{23}$$

For ISO internal threads, the relationship between a, b, c, and pitch P is

$$\begin{aligned} a &= 0.875P \\ b &= 0.5P \\ c &= 0.325P \end{aligned} \tag{24}$$

Substituting (24) into (9), (10), (11), (12), (13), (15), and (16) type one gets the relation

$$\delta_{1n} = 3.784\frac{M_{wn}}{E_n P^2 \beta_n^2} \cdot \left[\frac{1}{2}\left(\frac{1}{\beta_n^2}+1\right) - \frac{1}{\beta_n}\right] \cdot \frac{1}{(\beta_n - 1)^2}, \quad \beta_n = 1.751 \tag{25}$$

$$M_{wn} = \frac{w_z}{\mu\sin\alpha + \cos\alpha}\left[0.325P \cdot (\cos\alpha + \mu\cdot\sin\alpha) - (0.4375P - 0.325P\cdot\tan\alpha)(\sin\alpha - \mu\cdot\cos\alpha)\right] \tag{26}$$

$$\delta_{2n} = 0.55962 \cdot \frac{6(1+\nu)(\cos\alpha + \mu\sin\alpha)\cot\alpha}{5E_b} \cdot \frac{w_z}{\mu\sin\alpha + \cos\alpha} \tag{27}$$

$$\delta_{3n} = \frac{w_z}{\mu\sin\alpha + \cos\alpha} \cdot \frac{12c\left(1-\nu^2\right)}{\pi E_b a^2} \cdot \left[0.325P \cdot (\cos\alpha + \mu\cdot\sin\alpha) - (0.4375P - 0.325P\cdot\tan\alpha)(\sin\alpha - \mu\cdot\cos\alpha)\right] \tag{28}$$

$$\delta_{4n} = \left(\frac{D_0^2 + d_p^2}{D_0^2 - d_p^2} + \nu_n\right)\frac{d_p}{2E_n P} \cdot (\sin\alpha - \mu\cos\alpha)\tan\alpha \cdot \frac{w_z}{\mu\sin\alpha + \cos\alpha} \tag{29}$$

$$\delta_{5n} = \frac{1.7928 w_z}{\mu\sin\alpha + \cos\alpha} \cdot \frac{2\left(1-\nu^2\right)\cdot(\cos\alpha + \mu\sin\alpha)}{\pi E_b} \tag{30}$$

By adding these deformations separately, the total deformation (shown in Figure 4) of screw thread and nut thread can be obtained under the action of force w_z.

$$\delta_b = \delta_{1b} + \delta_{2b} + \delta_{3b} + \delta_{4b} + \delta_{5b} \tag{31}$$

$$\delta_n = \delta_{1n} + \delta_{2n} + \delta_{3n} + \delta_{4n} + \delta_{5n} \tag{32}$$

The unit force per unit width of the axial direction can be expressed as

$$f_\Delta = \frac{w_z}{w_z} = 1 \tag{33}$$

Under the action of unit force of axial unit width, the total deformation of external thread and internal thread is

$$\delta_{b1} = \frac{\delta_{1b} + \delta_{2b} + \delta_{3b} + \delta_{4b} + \delta_{5b}}{w_z} \tag{34}$$

and

$$\delta_{n1} = \frac{\delta_{1n} + \delta_{2n} + \delta_{3n} + \delta_{4n} + \delta_{5n}}{w_z} \tag{35}$$

For threaded connections, at the x-axis of the load F, the axial deformation of screws and nuts can be expressed as

$$z_b(r) = \delta_{b1} \cdot \frac{\partial F}{\partial r} \tag{36}$$

$$z_n(r) = \delta_{n1} \cdot \frac{\partial F}{\partial r} \tag{37}$$

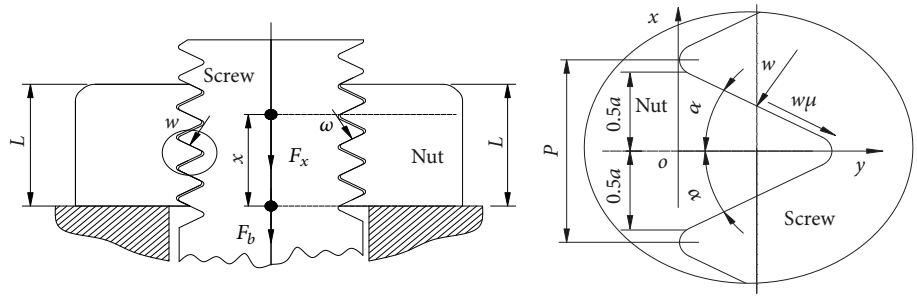

Thread axial force distribution (a) Partial view (b)

Figure 1: Thread force.

Here r is the length along the helical direction, and the relation between the axial height x and the length along the helix direction can be represented by the following formula according to the geometric relation shown in Figure 6.

$$r = \frac{x}{\sin\beta} \tag{38}$$

Here, β is the lead angle of the thread shown in Figure 6, and then

$$z_n(x) = \delta_{n1} \cdot \frac{\partial F}{\partial r} = \delta_{n1} \cdot \frac{\partial F}{\partial x} \cdot \frac{\partial x}{\partial r} = \delta_{n1} \cdot \sin\beta \cdot \frac{\partial F}{\partial x} \tag{39}$$

$$z_b(x) = \delta_{b1} \cdot \frac{\partial F}{\partial r} = \delta_{b1} \cdot \frac{\partial F}{\partial x} \cdot \frac{\partial x}{\partial r} = \delta_{b1} \cdot \sin\beta \cdot \frac{\partial F}{\partial x} \tag{40}$$

Assume

$$\frac{\partial F}{\partial x \cdot z_b(x)} = \frac{1}{\delta_{b1} \cdot \sin\beta} = k_{ubx}(x) \tag{41}$$

$$\frac{\partial F}{\partial x \cdot z_n(x)} = \frac{1}{\delta_{n1} \cdot \sin\beta} = k_{unx}(x) \tag{42}$$

Here, $k_{bx}(x)$ and $k_{nx}(x)$ represent the stiffness of the unit axial length of the nut and the screw, respectively, for the unit force.

The axial total deformation of the threaded connection at x is denoted as

$$z_x(x) = z_b(x) + z_n(x) \tag{43}$$

The stiffness of the unit axial length of the threaded connection is expressed as

$$\begin{aligned} k_{ux}(x) &= \frac{\partial F}{\partial x \cdot z_x(x)} \\ &= \frac{\partial F}{\partial x} \div \left(\delta_{b1} \cdot \sin\beta \cdot \frac{\partial F}{\partial x} + \delta_{n1} \cdot \sin\beta \cdot \frac{\partial F}{\partial x}\right) \\ &= \frac{1}{(\delta_{n1} + \delta_{b1}) \cdot \sin\beta} \end{aligned} \tag{44}$$

As shown in Figure 1(a), the threaded connection structure includes a nut body and a screw body. The nut is fixed, the screw is subjected to pulling force, the total axial force is F_b, and the axial force at the threaded connection screw x is $F(x)$. If the position of the bottom end face of the nut is the origin 0 and, at the x position, the axial force is $F(x)$, the screw elongation amount ε_b and the nut compression ε_n can be obtained from the following:

$$\varepsilon_b(x) = \frac{F(x)}{A_b(x) E_b} \tag{45}$$

$$\varepsilon_n(x) = \frac{F(x)}{A_n(x) E_n} \tag{46}$$

where $A_b(x)$ and $A_n(x)$ are the vertical cross-sectional areas of screws and nuts at the x position. E_b and E_n are, respectively, Young's modulus of the screw body and Young's modulus of the nut body. Find the displacement gradient for the expression, which is, respectively, expressed as

$$\frac{\partial z_b(x)}{\partial x} = \frac{1}{k_{ubx}(x)} \cdot \frac{\partial^2 F}{\partial x^2} \tag{47}$$

$$\frac{\partial z_n(x)}{\partial x} = \frac{1}{k_{unx}(x)} \cdot \frac{\partial^2 F}{\partial x^2} \tag{48}$$

Here, $k_{ubx}(x) = 1/(\delta_{b1} \cdot \sin\beta)$, and $k_{unx}(x) = 1/(\delta_{n1} \cdot \sin\beta)$.

As shown in Figure 1(a), the screw is subjected to the tensile force F_b, with the bottom of the nut as the coordinate origin, and the force at the x position is F_x, and then the elongation of the screw at x is $\int_x^L \varepsilon_b(x)dx = w_b$, and the compressed shortening amount of the nut at x is $\int_x^L \varepsilon_n(x)dx = w_n$. The relationship between w_b, w_n, z_b, and z_n is $\int_x^L \varepsilon_b(x)dx + \int_x^L \varepsilon_n(x)dx = [z_b(x) + z_n(x)]_{x=L} - [z_b(x) + z_n(x)]_{x=x}$ (see Figures 7 and 1(a),), and the partial derivative of this relation can be obtained by the following formula:

$$\varepsilon_b(x) + \varepsilon_n(x) = \frac{\partial z_b(x)}{\partial x} + \frac{\partial z_n(x)}{\partial x} \tag{49}$$

Substituting (45), (46), (47), and (48) into (49) and simplifying it

$$\frac{(A_n E_n + A_b E_b)}{A_b E_b A_n E_n} \cdot \frac{k_{ubx} k_{unx}}{(k_{ubx} + k_{unx})} F(x) = \frac{\partial^2 F(x)}{\partial x^2} \tag{50}$$

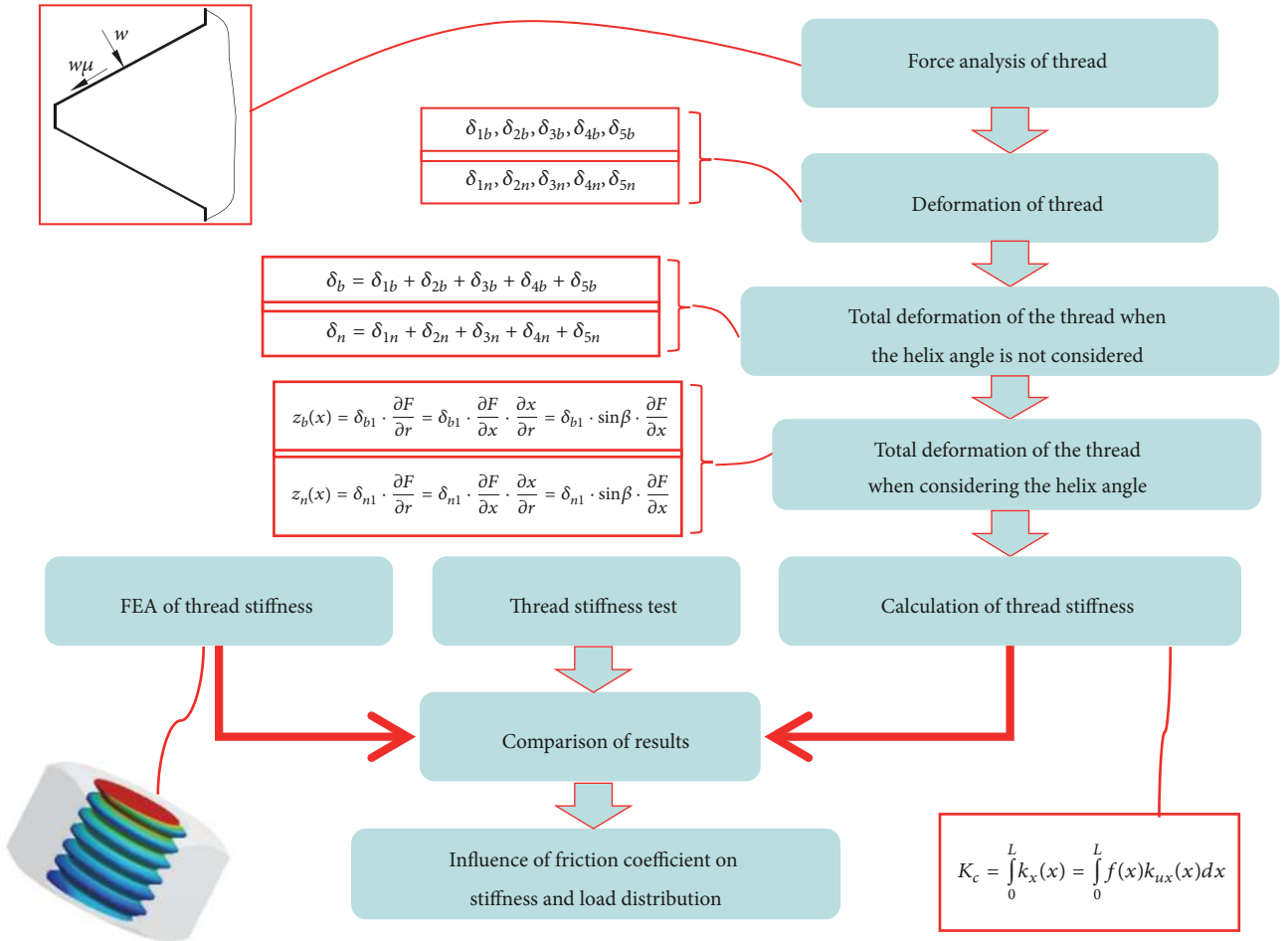

Figure 2: Schematic diagram of the article.

Let

$$n = \sqrt{\frac{(A_n E_n + A_b E_b)}{A_b E_b A_n E_n} \cdot \frac{k_{ubx} k_{unx}}{(k_{ubx} + k_{unx})}} \tag{51}$$

Then

$$n^2 F(x) = \frac{\partial^2 F(x)}{\partial x^2} \tag{52}$$

From mathematical knowledge, the equation is a differential equation. The general solution of the equation can be expressed as

$$F(x) = C_1 \sinh nx + C_2 \cosh nx \tag{53}$$

As can be seen from Figure 1, the axial force at the first thread at the connection surface of the nut and the screw is F_b, and the axial force at the last thread at the lower end of the thread joint surface of the nut and screw is 0; that is, the boundary condition is $F(x=0)=F_b$ and $F(x=L)=0$. Taking these boundary conditions into the equation will give $C_1=-F_b(\cosh(nL))/\sinh(nL)$ and $C_2=F_b$, so we get the expression of the threaded connection axial load as

$$F(x) = F_b \left(\cosh nx - \frac{\cosh nL}{\sinh nL} \sinh nx \right) \tag{54}$$

Therefore, the axial force distribution density of the thread connection along the x direction can be expressed as

$$f(x) = \frac{F(x)}{F_b} = \left(\cosh nx - \frac{\cosh nL}{\sinh nL} \sinh nx \right) \tag{55}$$

2.2. Thread Connection Stiffness. The stiffness in the axial direction x of the bolted connection is equal to the axial force distribution of the threaded connection multiplied by the unit stiffness; i.e.,

$$k_x(x) = f(x) k_{ux}(x) \tag{56}$$

The overall stiffness of the bolt connection can be expressed as

$$K_c = \int_0^L k_x(x) = \int_0^L f(x) k_{ux}(x) dx \tag{57}$$

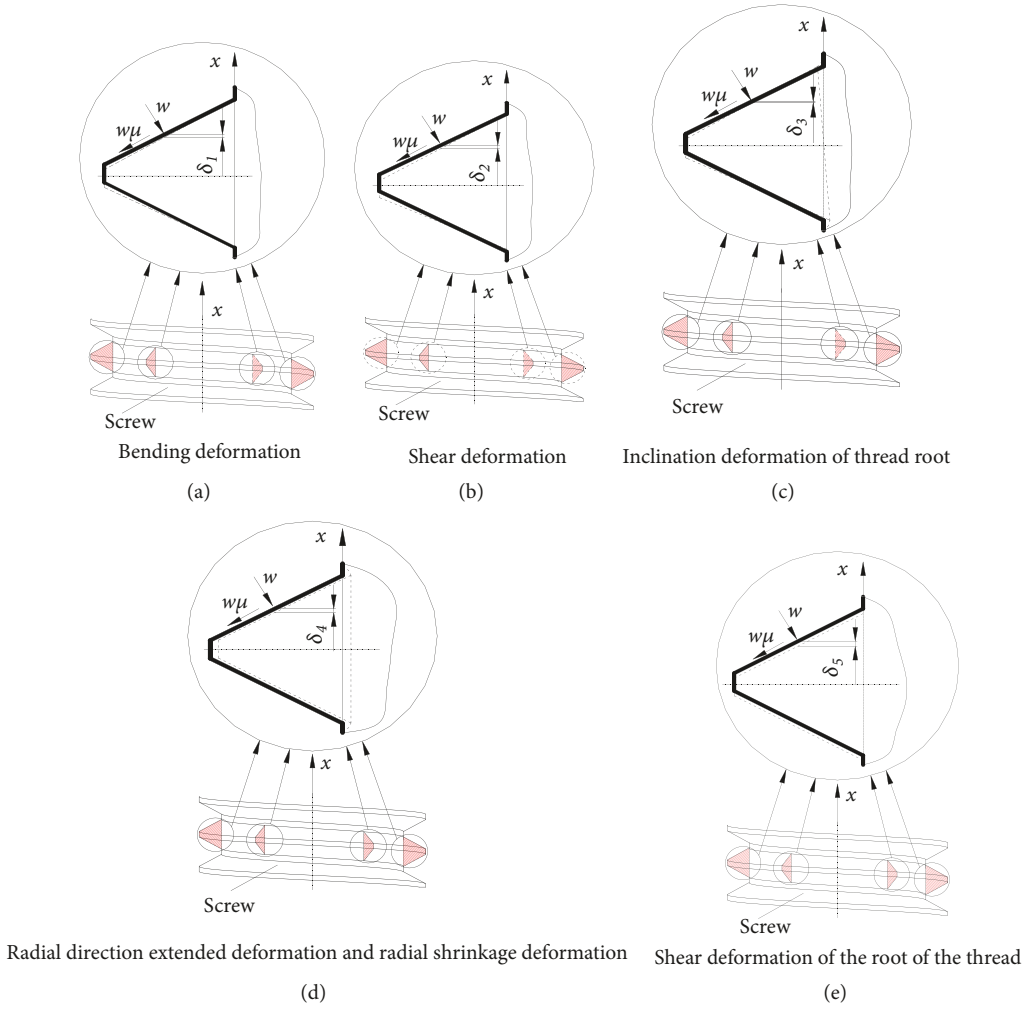

Figure 3: Thread deformation caused by various reasons.

Substituting (44) and (55) into (57), the stiffness of the bolt connection is expressed as

$$K_c = \int_0^L k_x(x) = \int_0^L f(x)\, k_{ux}(x)\, dx = \frac{1}{n(\delta_{b1} + \delta_{n1}) \cdot \sin\beta} \cdot \frac{\cosh nL - 1}{\sinh nL} \tag{58}$$

3. FEA Model

A 3D finite element model (shown in Figure 10) was established, and FEA was performed to analyze the influence of various parameters of the thread on the thread stiffness. These parameters include material, thread length, pitch, etc.

The FEA software ANSYS 14.0 was used for analysis. During the analysis, the end face of the nut was fixed (shown in Figure 9), the initial state of the model is shown in Figure 8, and an axial displacement Δ_x was forced to the end face of the screw. Then, the axial force F_x of the screw end face was extracted. The axial stiffness of the threaded connection was calculated by the FEM. The friction coefficient μ of the thread contact surface is set first. In FEA, the contact algorithm used is Augmented Lagrange. Figures 11(a)–11(c) are the force convergence curves for FEA of threaded connections. Figures 12(a)–12(c) are the effect of the reciprocal of the mesh size on the axial force obtained by FEA. We can see from Figures 12(a)–12(c) that as the mesh size decreases, the resulting axial force gradually decreases, but when the mesh size is small to a certain extent, the resulting axial force will hardly decrease. The axial force at this time is the axial force required by the author. With known displacements and axial force, the stiffness of the threaded connection can be calculated using the formula

$$K_c = \frac{F_x}{\Delta_x} \tag{59}$$

4. Tensile Test of Threaded Connections [1]

In order to verify the effectiveness of this paper method, the experimental data of the experimental device in [1] are used. In [1], the electronic universal testing machine is used to measure the load-defection data of samples, and the

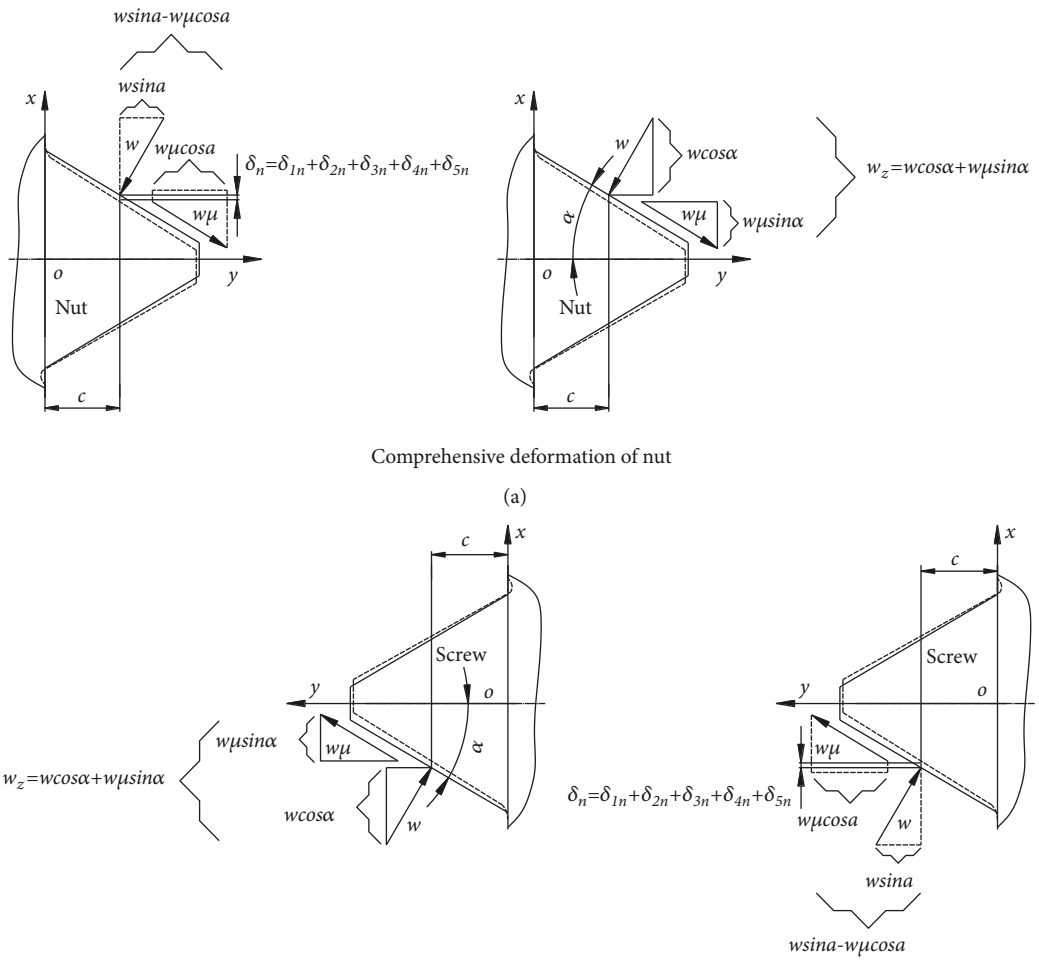

Figure 4: The comprehensive deformation of the thread.

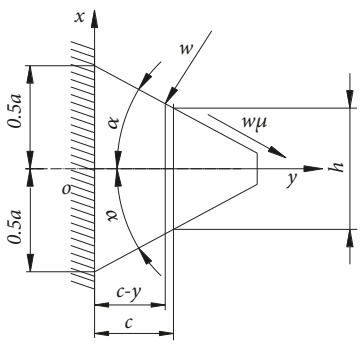

Figure 5: The force on the thread.

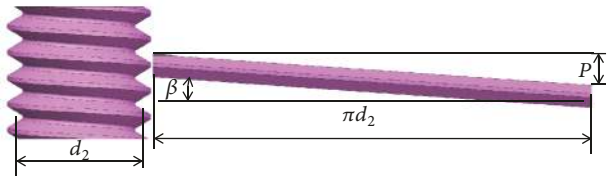

Figure 6: The lead angle of the thread.

test sample is made of brass. The tension value F_{xt} can be read from the test machine. The axial deflection of thread connection can be represented by the displacement variation δ_L between two lines as shown in Figure 14, which can be measured by a video gauge [1]. In [1], in order to obtain the most accurate data possible, each size of the thread is in a small range of deformation during the tensile test, and each size of the thread tensile test is performed 10 times, and the average value is calculated as the final calculated data. Some samples in the experiment are shown in Figure 13.

The stiffness calculation formula is

$$K_c = \frac{F_{xt}}{\delta_L}. \tag{60}$$

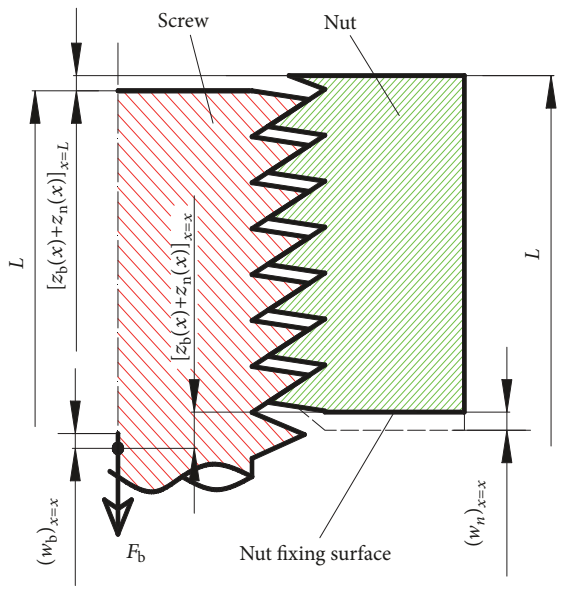

Figure 7: Illustration of the elastic deformation of the screwed portion of the threaded connection.

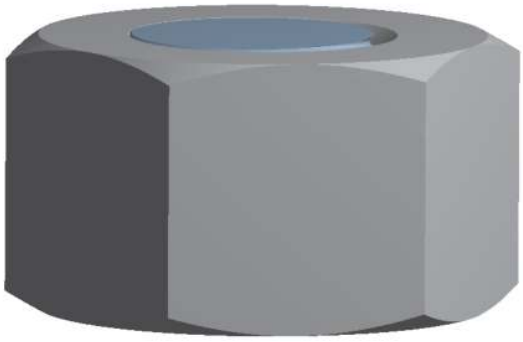

Figure 8: Initial state.

The materials used to make nuts and screws are brass. Young's modulus of brass is 107GPa, and Poisson's ratio is 0.32 [1].

5. Results and Discussion

5.1. Stiffness of Threaded Connections. Croccolo, D. [12], Nassar SA [19], and Zou Q [32] studied the coefficient of friction of the thread. According to the study by Zou Q and Nassar SA, in the case of lubricating oil on the thread surface, the friction coefficient of the steel-steel thread connection thread is 0.08, and the friction coefficient of aluminum-aluminum thread connection thread is 0.1.

In order to verify the correctness of the calculation results of the theory presented in this paper, a variety of threaded connections were used to calculate an experimental test.

In the finite element analysis and theoretical calculations of this paper, Young's modulus of steel is $E_b = E_n = 200$Gpa, and Poisson's ratio of steel is 0.3, and the friction coefficient [12, 19, 32] is set to 0.08.

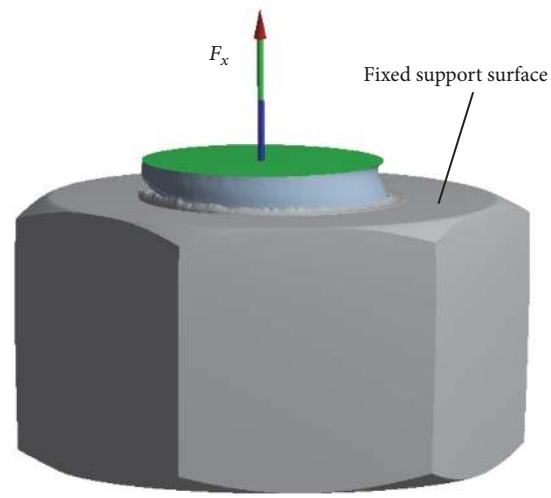

Figure 9: Threaded connection deformed by axial forces.

The experimental data, FEA data, and Yamamoto method data in Tables 1 and 5 are from literature [1]. As can be seen from Tables 1 and 5, the calculated values obtained in this paper are all higher than the experimental results. Perhaps the error is caused by the presence of a small amount of impurities on the surface of the thread and partial deformation of the thread inevitably and there is a slip between the threaded contact surfaces. The theoretical calculation results and FEA results in this paper have a small error.

In Table 2, the effect of thread length on stiffness is presented. It can be seen that when the same nominal diameter M10, the same pitch P=1.5, and the same material steel are taken, when the thread engaged length is taken as 14 mm, 9 mm, and 6 mm, respectively, it is found that the longer the thread engaged length, the greater the stiffness and the smaller the length of the bond, the smaller the stiffness.

In the FEA, the method of this paper and the Yamamoto method, Young's Modulus of aluminum alloy is E=68.9GPa; Poisson's ratio of the aluminum alloy is 0.34. The friction coefficient of the steel- steel threaded connection [12, 21, 22, 32] is set to 0.08, and the friction coefficient of aluminum-aluminum threaded connection [12, 19, 32] is set to 0.1. Table 3 shows the effect of different materials on the stiffness of threaded connections. The two types of threaded connections are made of two different materials, the steel and aluminum alloys. It can be seen from the table that, under the condition of the same pitch, the same nominal diameter, and the same engaged length, the stiffness of the steel thread connection is larger than that when the material is aluminum.

In Table 4, it also shows the influence of different pitches on the stiffness of the thread connection. It can be seen that with the same engaged length, the same material, and the same nominal diameter, the pitch P is 1.5, 1.25, and 1, respectively, and we find that the smaller the pitch, the greater the stiffness.

When using FEM to analyze the influence of friction factors on the stiffness of threaded connections, the thread

Table 1: Stiffness of threaded connections with different engaged lengths [1] (kN/mm).

No.	Size code of threads	Material	Exp.	Theory		FEA
				This study	Yamamoto method	
1	M36×4×32	Brass	3627.6	4201.9	4282.1	3630.9
2	M36×4×20		2664.3	3152.9	3946.1	2761.6
3	M36×4×12		1801.3	2074.2	3129.3	1816.8

(a) Nut (b) Screw

Figure 10: Finite element meshing of thread-bonded 3D finite element models.

Table 2: Stiffness of threaded connections with different engaged lengths (kN/mm).

No.	Size code of threads	Material	Theory		FEA
			This study	Yamamoto method	
1	M10×1.5×14	Steel	2095.26	2076.6	1965.21
2	M10×1.5×9		1759.23	2006.2	1770.02
3	M10×1.5×6		1354.70	1804.6	1551.27

Table 3: Stiffness of threaded connections with different material (kN/mm).

No.	Size code of thread	Material	Theory		FEA
			This study	Yamamoto method	
1	M10×1.5×9	Steel	1759.23	2006.2	1770.02
2	M10×1.5×9	Aluminum alloy	607.51	682.11	597.99

Table 4: Stiffness of threaded connections with different pitch (kN/mm).

No.	Size code of threads	Material	Theory	
			This study	Yamamoto method
1	M10×1.5×9	Steel	1759.23	2006.2
2	M10×1.25×9		2083.17	2177.1
3	M10×1×9		2324.30	2375.2

Table 5: Stiffness of threaded connections with different engaged lengths [1] (kN/mm).

No.	Size code of threads	Material	Exp.	Theory	
				This study	Yamamoto method
1	M36×3×12	Brass	2085.3	2593.2	3525.1
2	M36×2×12	Brass	2396.2	3418.3	4008.9

specification is M6×1×6.1 and the friction coefficients are 0.01, 0.05, 0.1, 0.2, 0.25, and 0.3. (as shown in Figures 15–20)

Figures 21 and 22 show the results of stiffness calculations. The thread size is M10×1.5×9 and M6×1×6.1, the material is steel, Poisson's ratio of the material is 0.3, Young's Modulus of the material is 200 GPa, and the thread surface friction coefficient is taken as 0.01, 0.05, 0.1, 0.2, 0.25, and 0.3. Calculated using the theories of this paper, FEA and Yamamoto, respectively, and from Figures 21 and 22, we can see that the results of FEA are very similar to the results of the theoretical calculations of this paper, the variation trend of stiffness with friction coefficient is the same, and it increases with the increase of friction coefficient, and the results of the FEA are in good agreement with those of the FEA;

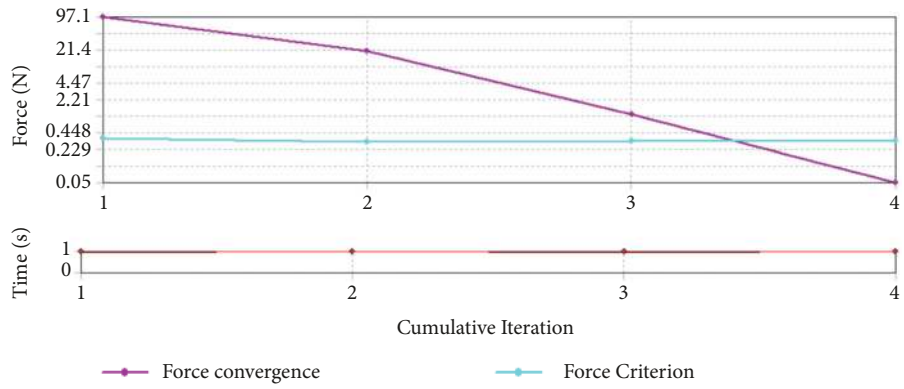

(a) M10×1.5×9, μ=0.08, Δ_x=0.001mm

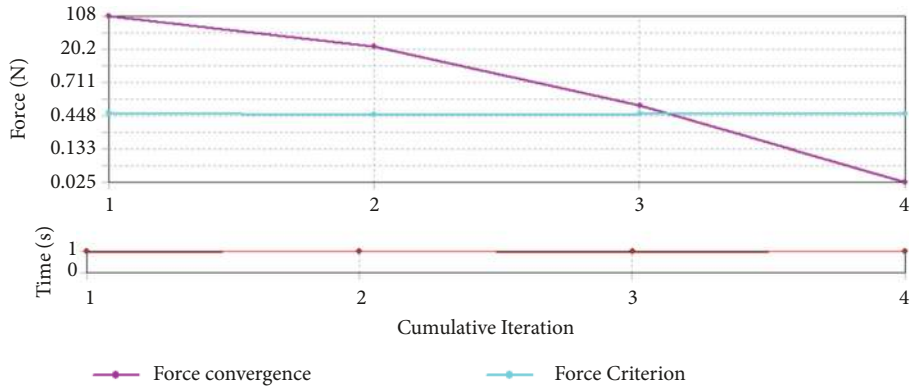

(b) M8×1.25×6.5, μ=0.08, Δ_x=0.001mm

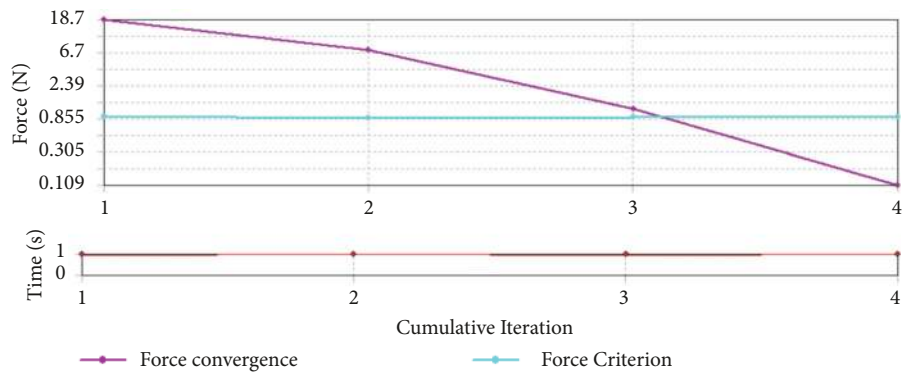

(c) M6×1.0×6.1, μ=0.08, Δ_x=0.001mm

Figure 11: FEA convergence curve.

however, Yamamoto theory does not consider the influence of the friction coefficient on stiffness, and this is obviously unreasonable.

5.2. Effect of Friction Coefficient on Axial Force Distribution. Take the thread size as M6×0.75×6.1, the axial load F_b is taken as 100N, 350N, and 550N, respectively, and take the friction coefficients 0, 0.3, 0.6, and 1, respectively, to calculate the axial force distribution of the thread. As can be seen from Figure 23, when the friction coefficient is 1, the curve bending degree is the greatest, when the friction coefficient is 0, the curve bending degree is the lightest, the curve bending degree is greater, indicating that the more uneven the distribution of axial force, the smaller the curve bending degree, indicating that the more uniform the distribution of axial force. We can see that the friction coefficient of thread surface has an effect on the distribution of axial force.

6. Conclusion

This study provides a new method of calculating the thread stiffness considering the friction coefficient and analyzes the influence of the thread geometry and material parameters on the thread stiffness and also analyzes the influence of

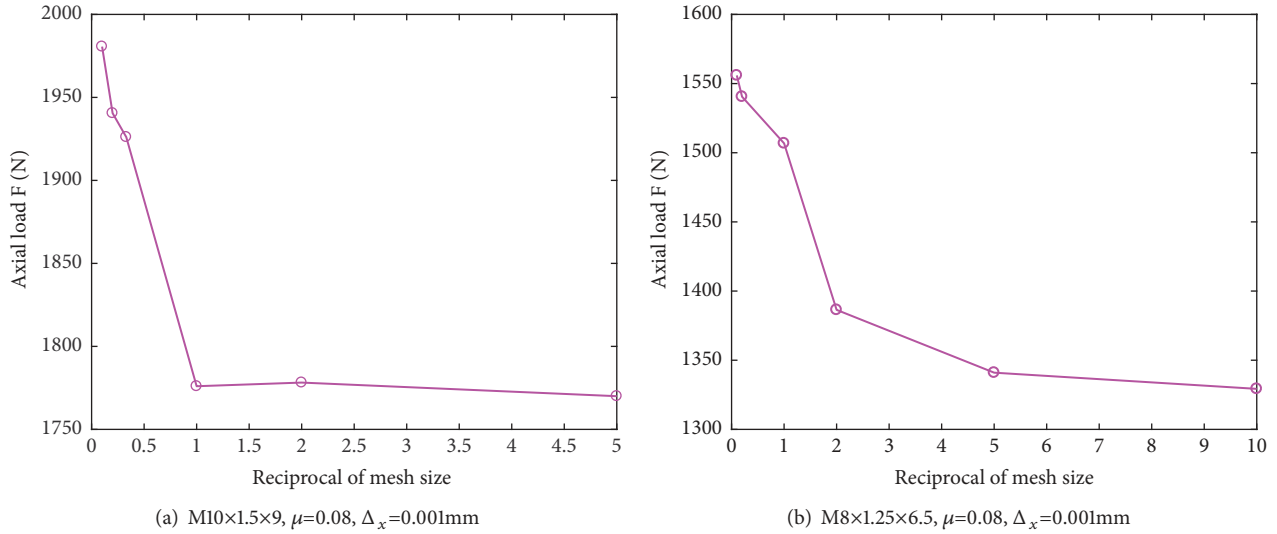

(a) M10×1.5×9, μ=0.08, Δ_x=0.001mm

(b) M8×1.25×6.5, μ=0.08, Δ_x=0.001mm

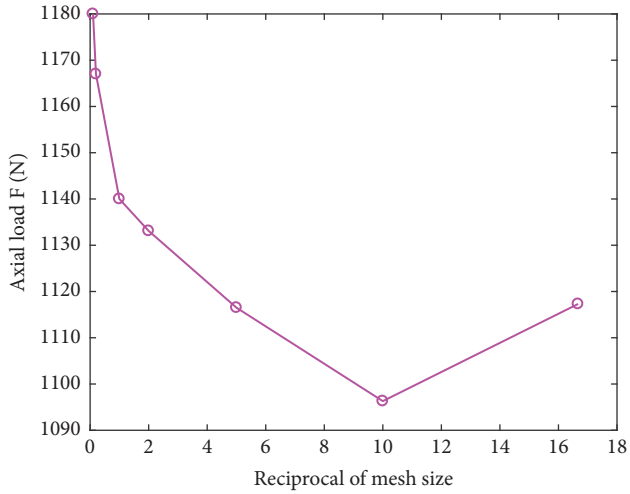

(c) M6×1.0×6.1, u=0.08, Δ_x=0.001mm

Figure 12: Influence of the reciprocal of finite element mesh size on axial force.

the friction coefficient on the thread stiffness and axial force distribution.

(1) The results of the calculation of the thread stiffness calculated by the theoretical calculation method of this study are basically consistent with the results of the FEA. The results obtained by the test are smaller than the calculated results. This is due to the influence of the thread manufacturing on the experimental results.

(2) Thread-stiffness is closely related to material properties, pitch, and thread length. We can obtain higher stiffness by increasing Young's modulus of the material, increasing the length of the thread, and reducing the pitch.

(3) We can also increase the friction coefficient of the thread joint surface to increase the stiffness of the thread connection, but we have found that using this method to increase the thread stiffness is limited.

(4) In order to make the axial load distribution of the thread uniform, we can reduce the friction coefficient of the thread surface, but we found that the use of this method to improve the distribution of the axial force of the thread has limited effectiveness.

Nomenclature

μ: Contact surface friction coefficient
w_z: Axial unit width force, N
δ_1: Thread bending deformation, mm
δ_2: Thread shear deformation, mm
δ_3: Thread root inclination deformation, mm
δ_4: Radial direction extended deformation or radial shrinkage deformation, mm
δ_5: Thread root shear deformation, mm
$\overline{E}$: Bending moment of the unit load beam, N•mm

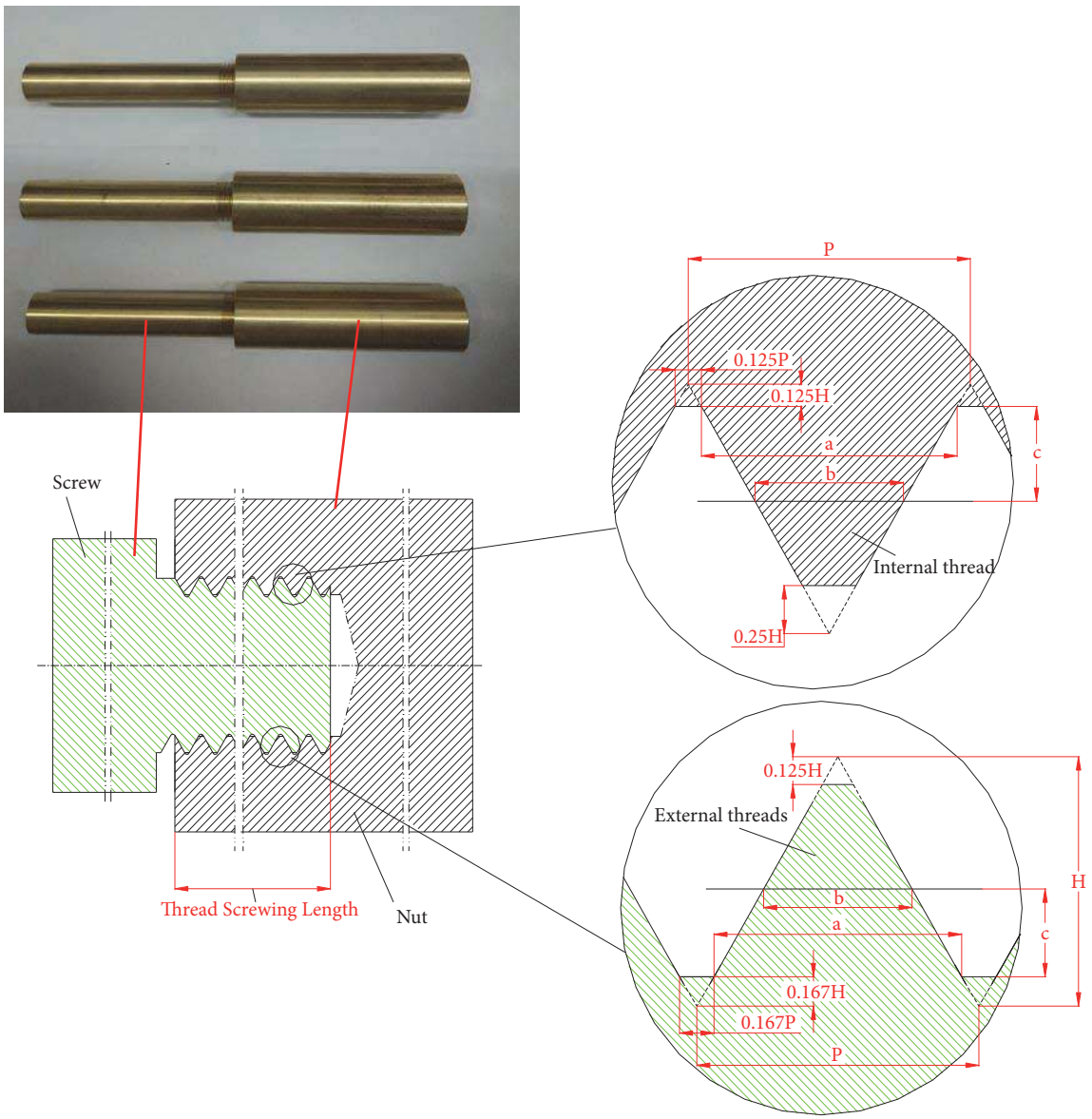

Figure 13: Part of experimental threaded connection samples and ISO internal thread and ISO external thread.

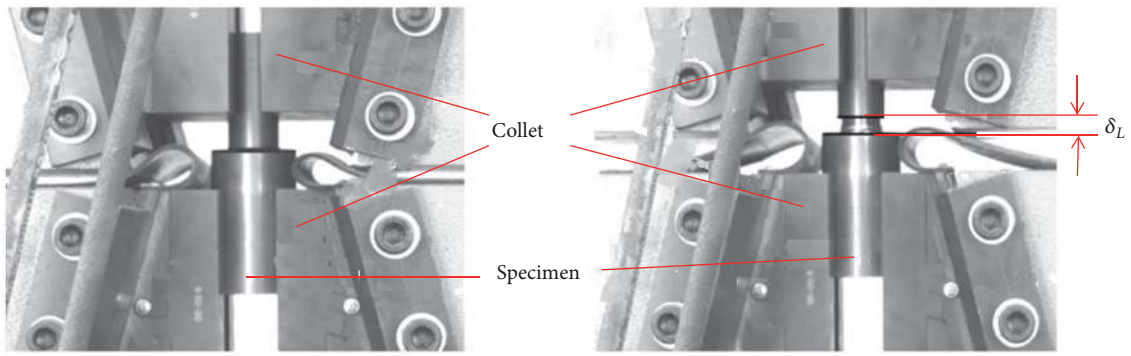

Figure 14: Tensile test [1].

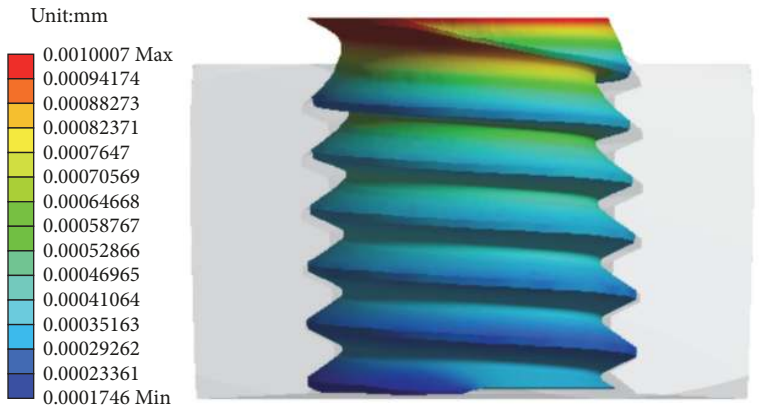

Figure 15: Axial displacement for screws with a friction coefficient of μ=0.01. Total force reaction=1086.00 N.

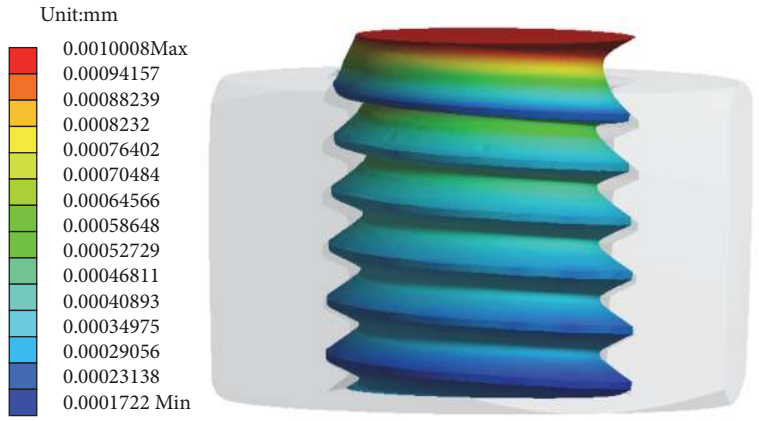

Figure 16: Axial displacement for screws with a friction coefficient of μ=0.05. Total force reaction=1092.00 N.

M_w: Bending moment of the beam under the actual load, N•mm
I: Area moment of inertia, mm^4
E_b: Young's modulus of the screw material, N/mm^2
c: Length of the beam, thread pitch line height, mm
h: Beam end section height, mm
B: Beam section width, mm
β_1: Beam root section height and the beam end section height ratio
B_b: Ratio of the height of the screw thread root section to the section height at the middiameter
B_n: Ratio of the height of the nut thread root section to the section height at the middiameter
δ_{4b}: Radial shrinkage deformation of the screw thread, mm
δ_{4n}: Radial direction extended deformation of the nut thread, mm
a: Width of the thread root, mm
D_0: Cylinder (nut) outer diameter, mm
d_p: Effective diameter of the thread, mm
ν_n: Poisson's ratio of nut material
P: Pitch, mm
M_{wb}: Bending moment of the screw thread, N•mm
δ_{1b}: Thread bending deformation of the screw thread, mm
δ_{2b}: Thread shear deformation of the screw thread, mm
δ_{3b}: Thread root inclination deformation of the screw thread, mm
δ_{4b}: Radial direction extended deformation of the screw thread, mm
δ_{5b}: Thread root shear deformation of the screw thread, mm
M_{wn}: Bending moment of the nut thread, N•mm
δ_{1n}: Thread bending deformation of the nut thread, mm
δ_{2n}: Thread shear deformation of the nut thread, mm
δ_{3n}: Thread root inclination deformation of the nut thread, mm
δ_{4n}: Radial direction extended deformation of the nut thread, mm
δ_{5n}: Thread root shear deformation of the nut thread, mm
f_Δ: Unit force per unit width of the axial direction

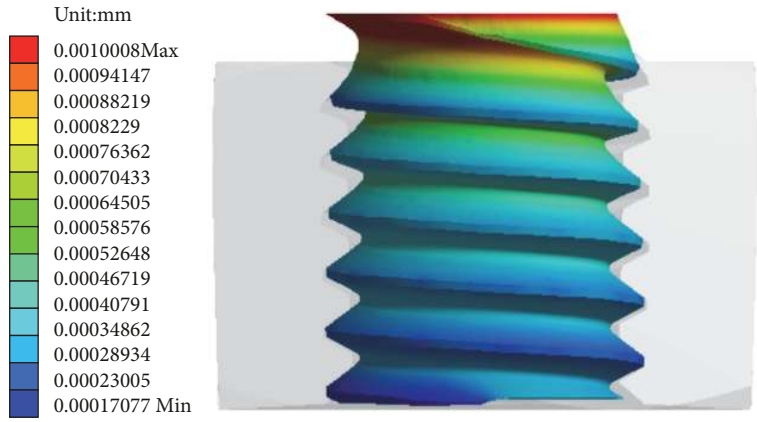

Figure 17: Axial displacement for screws with a friction coefficient of μ=0.1. Total force reaction=1098.00 N.

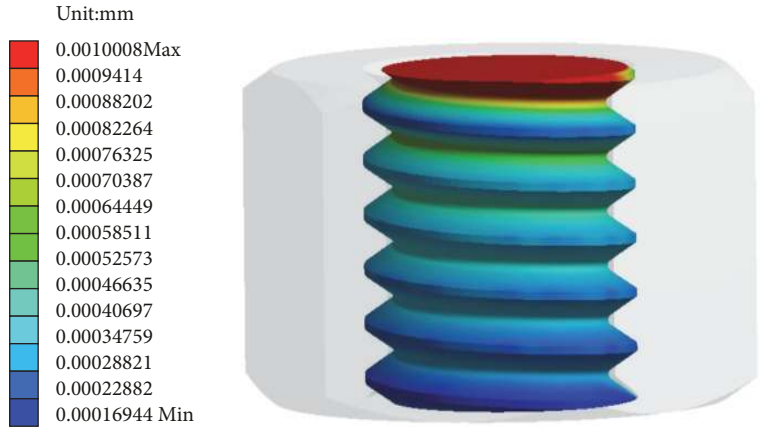

Figure 18: Axial displacement for screws with a friction coefficient of μ=0.2. Total force reaction=1108.40 N.

δ_{b1}: Total deformation of external (screw) thread, mm
δ_{n1}: Total deformation of internal (nut) thread, mm
z_b: The load on somewhere on the x-axis is F, where the screw thread axial deformation, mm
z_n: The load on somewhere on the x-axis is F, where the nut thread axial deformation, mm
r: Length along the helical direction, mm
β: Lead angle of the thread, degree
$k_{bx}(x)$: Stiffness of the unit axial length of the screw, N/mm
$k_{nx}(x)$: Stiffness of the unit axial length of the nut, N/mm^2
z_x: Axial total deformation of the threaded connection, mm
$k_{ux}(x)$: Stiffness of the unit axial length of the threaded connection, N/mm^2
F_b: Total axial force (load), N
ε_b: At the x position, the axial force is $F(x)$, the screw elongation amount
ε_n: At the x position, the axial force is $F(x)$, the nut compression amount
$A_b(x)$: Vertical cross-sectional areas of screw at the x position, mm^2
$A_n(x)$: Vertical cross-sectional areas of nut at the x position, mm^2
E_b: Young's modulus of the screw body, N/mm^2
E_n: Young's modulus of the nut body, N/mm^2
$k_x(x)$: Stiffness in the axial direction x, N/mm
K_c: Overall stiffness of the threaded connection, N/mm
Δ_x: Axial displacement, mm
F_x: Total axial force, N
F_{xt}: Axial tension load, N
K_t: Overall stiffness of the threaded connection, N/mm

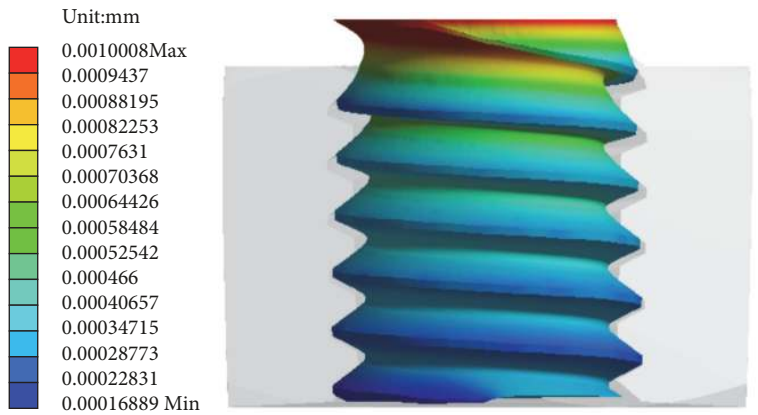

Figure 19: Axial displacement for screws with a friction coefficient of μ=0.25. Total force reaction=1110.6 N.

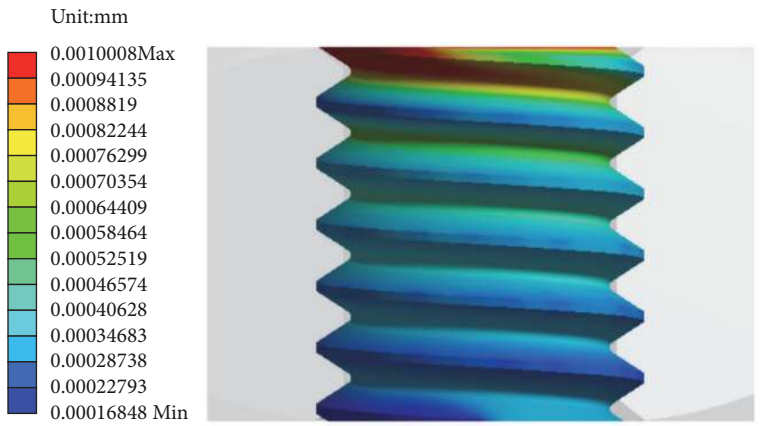

Figure 20: Axial displacement for screws with a friction coefficient of μ=0.3. Total force reaction=1114.2 N.

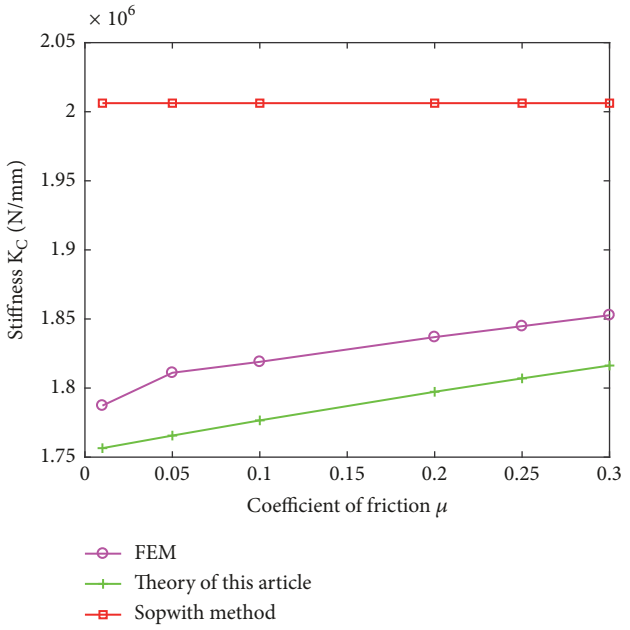

Figure 21: Effect of friction coefficient on stiffness. M10×1.5×9.

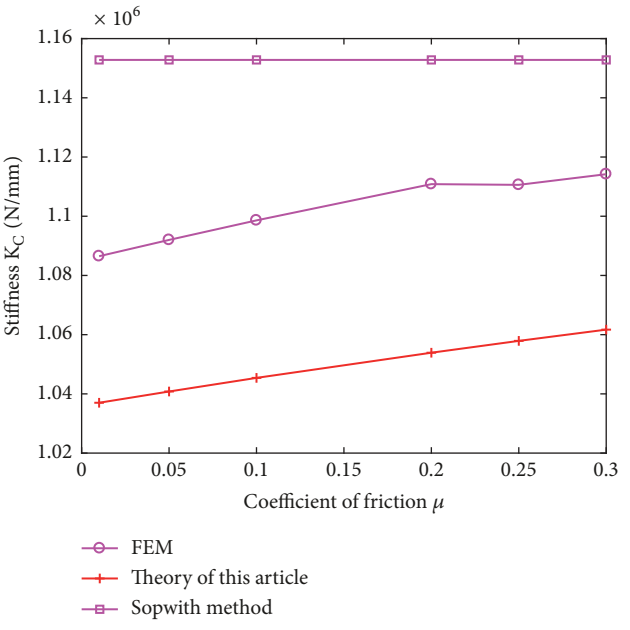

Figure 22: Effect of friction coefficient on stiffness. M6×1×6.1.

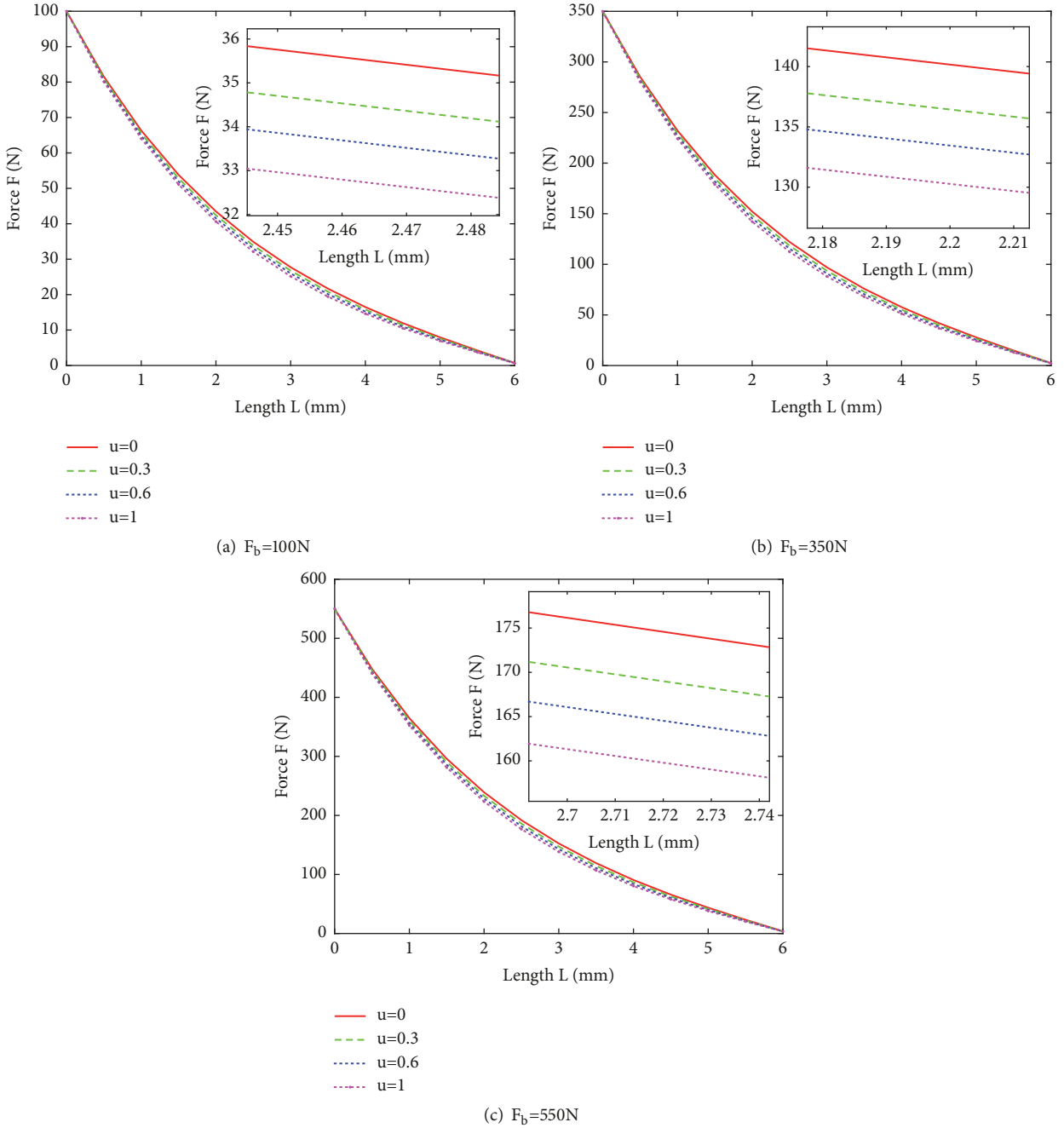

(a) F_b=100N

(b) F_b=350N

(c) F_b=550N

Figure 23: Effect of Friction Coefficient on Axial Force Distribution.

δ_L: Axial deformation of the thread, mm
H: Thread original triangle high, mm.

Data Availability

The data used to support the findings of this study are included within the article.

Conflicts of Interest

The authors declare that they have no conflicts of interest.

Acknowledgments

The authors would like to acknowledge support from the National Natural Science Foundation of China [Grant nos. 51675422, 51475366, and 51475146] and Science &

Technology Planning Project of Shaanxi Province [Grant no. 2016JM5074].

References

[1] D. Zhang, S. Gao, and X. Xu, "A new computational method for threaded connection stiffness," *Advances in Mechanical Engineering*, vol. 8, no. 12, 2016.

[2] K. Murayama, I. Yoshimoto, and Y. Nakano, "On spring constant of bolted joints," *Transactions of the Japan Society of Mechanical Engineers*, vol. 41, no. 344, pp. 1289–1297, 1975.

[3] I. Fernlund, *A Method to Calculate the Pressure Between Bolted or TU, 1962. Riveted Plates*, Chalmers University of Technology, 1961.

[4] N. Motosh, "Determination of joint stiffness in bolted connections," *Journal of Engineering for Industry*, vol. 98, no. 3, pp. 858–861, 1976.

[5] B. Kenny and E. A. Patterson, "Load and stress distribution in screw threads," *Experimental Mechanics*, vol. 25, no. 3, pp. 208–213, 1985.

[6] B. Kenny and E. A. Patterson, "The distribution of load and stress in the threads of fasteners - a review," *Journal of the Mechanical Behavior of Materials*, vol. 2, no. 1-2, pp. 87–106, 1989.

[7] D. L. Miller, K. M. Marshek, and M. R. Naji, "Determination of load distribution in a threaded connection," *Mechanism and Machine Theory*, vol. 18, no. 6, pp. 421–430, 1983.

[8] W. Wang and K. M. Marshek, "Determination of load distribution in a threaded connector with yielding threads," *Mechanism and Machine Theory*, vol. 31, no. 2, pp. 229–244, 1996.

[9] J. Wileman, M. Choudhury, and I. Green, "Computation of member stiffness in bolted connections," *Journal of Mechanical Design*, vol. 113, no. 4, pp. 432–437, 1991.

[10] M. De Agostinis, S. Fini, and G. Olmi, "The influence of lubrication on the frictional characteristics of threaded joints for planetary gearboxes," *Proceedings of the Institution of Mechanical Engineers, Part C: Journal of Mechanical Engineering Science*, vol. 230, no. 15, pp. 2553–2563, 2016.

[11] D. Croccolo, M. De Agostinis, S. Fini, and G. Olmi, "Tribological properties of bolts depending on different screw coatings and lubrications: An experimental study," *Tribology International*, vol. 107, pp. 199–205, 2017.

[12] D. Croccolo, M. De Agostinis, S. Fini, and G. Olmi, "An experimental study on the response of a threadlocker, involving different materials, screw dimensions and thread proportioning," *International Journal of Adhesion and Adhesives*, 2018.

[13] D. Croccolo, M. De Agostinis, and N. Vincenzi, "Failure analysis of bolted joints: Effect of friction coefficients in torque-preloading relationship," *Engineering Failure Analysis*, vol. 18, no. 1, pp. 364–373, 2011.

[14] Q. Zou, T. S. Sun, S. A. Nassar, G. C. Barber, and A. K. Gumul, "Effect of lubrication on friction and torque-tension relationship in threaded fasteners," in *Proceedings of the STLE/ASME International Joint Tribology Conference (IJTC '06)*, San Antonio, TX, USA, October 2006.

[15] Q. Zou, T. S. Sun, S. Nassar, G. C. Barber, H. El-Khiamy, and D. Zhu, "Contact mechanics approach to determine effective radius in bolted joints," *Journal of Tribology*, vol. 127, no. 1, pp. 30–36, 2005.

[16] S. A. Nassar, P. H. Matin, and G. C. Barber, "Thread friction torque in bolted joints," *Journal of Pressure Vessel Technology*, vol. 127, no. 4, pp. 387–393, 2005.

[17] S. A. Nassar, H. El-Khiamy, G. C. Barber, Q. Zou, and T. S. Sun, "An experimental study of bearing and thread friction in fasteners," *Journal of Tribology*, vol. 127, no. 2, pp. 263–272, 2005.

[18] S. A. Nassar, G. C. Barber, and D. Zuo, "Bearing friction torque in bolted joints," *Tribology Transactions*, vol. 48, no. 1, pp. 69–75, 2005.

[19] S. Nassar A, S. Ganeshmurthy, R. Ranganathan M et al., "Effect of tightening speed on the torque-tension and wear pattern in bolted connections," *Journal of Pressure Vessel Technology*, vol. 129, no. 3, pp. 1669–1681, 2007.

[20] H. Kopfer, C. Friedrich, M. De Agostinis, and D. Croccolo, "Friction characteristics in light weight design focusing bolted joints," in *Proceedings of the ASME International Mechanical Engineering Congress and Exposition (IMECE '12)*, pp. 839–846, November 2012.

[21] B. Kenny and E. A. Patterson, "The distribution of load and stress in the threads of fasteners - a review," *Journal of the Mechanical Behavior of Materials*, vol. 2, no. 1-2, pp. 87–105, 1989.

[22] J. E. Shigley, C. R. Mischke, and R. G. Budynas, *Mechanical Engineering Design*, McGraw-Hill, New York, NY, USA, 2004.

[23] T. F. Lehnhoff and W. E. Wistehuff, "Nonlinear effects on the stresses and deformations of bolted joints," *Journal of Pressure Vessel Technology, Transactions of the ASME*, vol. 118, no. 1, pp. 54–58, 1996.

[24] N. S. Al-Huniti, "Computation of member stiffness in bolted connections using the finite element analysis," *Mechanics Based Design of Structures and Machines*, vol. 33, no. 3-4, pp. 331–342, 2005.

[25] J. C. Musto and N. R. Konkle, "Computation of member stiffness in the design of bolted joints," *Journal of Mechanical Design*, vol. 128, no. 6, pp. 1357–1360, 2006.

[26] N. Haidar, S. Obeed, and M. Jawad, "Mathematical representation of bolted-joint stiffness: A new suggested model," *Journal of Mechanical Science and Technology*, vol. 25, no. 11, pp. 2827–2834, 2011.

[27] S. A. Nassar and A. Abboud, "An improved stiffness model for bolted joints," *Journal of Mechanical Design*, vol. 131, no. 12, Article ID 121001, 2009.

[28] Z. Y. Qin, Q. K. Han, and F. L. Chu, "Analytical model of bolted disk-drum joints and its application to dynamic analysis of jointed rotor," *Proceedings of the Institution of Mechanical Engineers, Part C: Journal of Mechanical Engineering Science*, vol. 228, no. 4, pp. 646–663, 2014.

[29] J. Liu, H. Ouyang, J. Peng et al., "Experimental and numerical studies of bolted joints subjected to axial excitation," *Wear*, vol. 346-347, pp. 66–77, 2016.

[30] D. G. Sopwith, "The distribution of load in screw threads," *Proceedings of the Institution of Mechanical Engineers*, vol. 159, no. 1, pp. 373–383, 2006.

[31] A. Yamamoto, *The Theory and Computation of Threads Connection*, Yokendo, Tokyo, Japan, 1980.

[32] Q. Zou, T. S. Sun, S. A. Nassar, G. C. Barber, and A. K. Gumul, "Effect of lubrication on friction and torque-tension relationship in threaded fasteners," *Tribology Transactions*, vol. 50, no. 1, pp. 127–136, 2007.